Disentangling α and β relaxation in orientationally disordered crystals with theory and experiments

Bingyu Cui,[1] Jonathan F. Gebbia,[3] Josep-Lluis Tamarit,[3] and Alessio Zaccone[1,2]

[1]*Statistical Physics Group, Department of Chemical Engineering and Biotechnology, University of Cambridge, Philippa Fawcett Drive, CB3 0AS Cambridge, United Kingdom*

[2]*Cavendish Laboratory, University of Cambridge, JJ Thomson Avenue, CB3 0HE Cambridge, United Kingdom*

[3]*Grup de Caracterizacio de Materials, Departament de Fisica, EEBE, Barcelona Research Center in Multiscale Science and Engineering, Universitat Politecnica de Catalunya, Eduard Maristany, 10-14, 08019 Barcelona, Catalonia*

(Received 8 March 2018; published 21 May 2018)

We use a microscopically motivated generalized Langevin equation (GLE) approach to link the vibrational density of states (VDOS) to the dielectric response of orientational glasses (OGs). The dielectric function calculated based on the GLE is compared with experimental data for the paradigmatic case of two OGs: freon-112 and freon-113, around and just above T_g. The memory function is related to the integral of the VDOS times a spectral coupling function $\gamma(\omega_p)$, which tells the degree of dynamical coupling between molecular degrees of freedom at different eigenfrequencies. The comparative analysis of the two freons reveals that the appearance of a secondary β relaxation in freon-112 is due to cooperative dynamical coupling in the regime of mesoscopic motions caused by stronger anharmonicity (absent in freon-113) and is associated with the comparatively lower boson peak in the VDOS. The proposed framework brings together all the key aspects of glassy physics (VDOS with the boson peak, dynamical heterogeneity, dissipation, and anharmonicity) into a single model.

DOI: 10.1103/PhysRevE.97.053001

I. INTRODUCTION

Structural glass (SG) formers, which are usually obtained from supercooled liquids in which translational and orientational degrees of freedom are frozen below the glass transition temperature T_g, exhibit a complex response function on vibrational excitations [1–4]. When they undergo a rapid cooling to avoid crystallization, some anomalous physical properties emerge. For example, as temperature decreases, the relaxation time generally shows a stronger increase, faster than what is given by the Arrhenius law (super-Arrhenius behavior). For such cases, the temperature (T) dependence of relaxation time (τ) is given through the empirical Vogel-Fulcher-Tammann law [5,6] or by physically motivated double-exponential dependence of τ on T, which includes the dependence on the steepness of interatomic repulsion and on thermal expansion via the more recent Krausser-Samwer-Zaccone relation [7]. To account for the deviation of the Arrhenius temperature dependence, i.e., for the faster increase in the relaxation time (or viscosity), the kinetic fragility index is defined as $m = \frac{\partial \log_{10} \tau}{\partial(T_g/T)}|_{T=T_g}$, ranging between $\approx$16 (strong glasses) and 200 (fragile glasses) [8,9].

In addition to the structural glasses, orientational glasses (OGs) can be obtained from orientationally disordered (OD) phases or plastic phases [10–12]. OD phases are crystal lattices in which weakly interacting molecules are orientationally disordered. On cooling, some OD phases exhibit the same features as structural (canonical) glass formers [11,13–15]. With respect to the fragility index, OGs are usually strong [8], whereas for SGs a wide range of fragility values are found, the most fragile being the *cis*- or *trans*-decahydronaphthalene ($m \approx$ 147) [16]. The most fragile OGs known to date include freon-112 [CCl_2F-CCl_2F, hereinafter (F112)] with $m = 68$ [15]. On the other hand, for freon-113 [CCl_2F-$CClF_2$, hereinafter (F113)], the kinetic fragility index was calculated to be $m =$ 127, which is the highest so far reported for an OG [17].

In an effort to explain the various glassy anomalies and dynamical behavior, mode-coupling theory provides, among other predictions, a good description for the dielectric relaxation of liquids for temperatures higher than the liquid crossover temperature T_c [18]. Despite this, the main relaxation mechanism by which supercooled liquids undergo a liquid-solid transition, at or around T_g, has remained elusive [19]. The α relaxation, typically associated with collective and strong cooperative motions of a large number of entities rearranging in a long-range correlated way, is related to the slowest decay of density correlations and is widely observed in dielectric and mechanical responses.

For supercooled liquids, the empirical Kohlrausch stretched-exponential function $\sim \exp[-(t/\tau)^{\beta}]$ provides a good empirical fit for the dielectric loss of the α relaxation upon taking the Fourier transform from the time into the frequency domain. Furthermore, starting from the first principles assumption that the microscopic Hamiltonian can be modeled using a classical particle-bath coupling of the Caldeira-Leggett type, a simple and explicit relation between the dielectric relaxation function and the vibrational density of states (VDOS) of the SGs has been presented to provide a good interpretation of the α peak and stretched-exponential relaxation through a memory function of friction [20].

In addition to α relaxation, an extra shoulder or wing also decorates the imaginary part of the dielectric response, which is referred to as the β relaxation, as Johari-Goldstein, or as the secondary relaxation. As discovered by Johari and Goldstein [21] in glasses of rigid molecules and as described by the Ngai coupling model [22], the secondary relaxation involves the

motion of the entire molecule. Knowing the underlying mechanism of β relaxation is of great importance for understanding many crucial unresolved issues in glassy physics and materials science and consequently for a wide potential application in technologies, ranging from glass transitions and deformation mechanisms to diffusion and the breakdown of the Stokes-Einstein relations, physical aging, as well as the conductivity of ionic liquids and the stability of glassy pharmaceuticals and biomaterials. Yet, the nature and mechanism of the β relaxations are still not clear [23–26].

In order to understand the puzzling origin of the β relaxation it is instructive to consider systems with very similar molecular structures and yet exhibiting widely different relaxation behaviors. Such systems can be found in the realm of OGs.

Previous study on thermal conductivities of F112 and F113 reveals the existence of quasilocalized low-energy vibrational modes (soft harmonic oscillators as described through the soft potential model [27]) at energies lower than the values of the maximum of the boson peak compared with other OGs, which results in an increase in the VDOS [13]. It was thought that the high values of kinetic ($m = 127$) fragility of F113 are produced by strong orientational correlations, which is evidenced by low values of the stretching exponent in the Kohlrausch stretched-exponential function close to T_g where only α relaxation is observed with no sign of the β relaxation. On the contrary, in dielectric spectra of F112, β relaxation emerges as temperature decreases to T_g and becomes evident below T_g.

The above experimental facts are the origin of our interest in applying a microscopic theoretical model to plastic crystals. In particular, freons F112 and F113 are chemically and molecularly similar compounds displaying glassy states (they both belong to the series $C_2X_{(6-n)}Y_n$ with $X,Y = $ Cl, F, Br, and $n = 0,\ldots,6$) but with completely different dynamics and relaxation. This provides a unique opportunity to explain, from a microscopic point of view, the physical origin of secondary β relaxation.

We therefore developed a modified theoretical model in the spirit of Ref. [20] to account for both α and β relaxations, and we apply it to OG states of freons F112 and F113. From the analysis of experimental data, it is evident that: (i) The proposed generalized Langevin equation (GLE) theory successfully describes both α- and β-relaxation processes in the dielectric response by using the experimentally measured VDOS as input; (ii) the model provides a different insight into the dynamical origin of the secondary relaxation; (iii) the model also clarifies which eigenmodes dynamically couple with the secondary relaxation process. This framework presents a microscopic model of the glassy relaxation in orientationally disordered crystals for which no theoretical framework existed so far.

II. THEORY

Focusing on a tagged particle (e.g., a molecular subunit carrying a partial charge which reorients under the electric field), it is possible to describe its motion under the applied field using a particle-bath Hamiltonian of the Caldeira-Leggett type in the classical dynamics regime [20]. The particle's Hamiltonian is bilinearly coupled to a bath of harmonic oscillators which represent all other molecular degrees of freedom in the system [28]. Any complex system of oscillators can be reduced to a set of independent oscillators by performing a suitable normal-mode decomposition. This allows us to identify the spectrum of eigenfrequencies of the system, i.e., the experimental VDOS, with the spectrum of the set of harmonic oscillators forming the bath.

A. Particle-bath Hamiltonian and GLE

The particle-bath Hamiltonian under a uniform ac electric field is given by [20] $H = H_P + H_B$ where $H_P = P^2/2m + V(Q) - q_e Q E_0 \sin(\omega t)$ is the Hamiltonian of the tagged particle with the external electric field (q_e is the charge carried by the particle) and $H_B = \frac{1}{2}\sum_{\alpha=1}^{N}[\frac{P_\alpha^2}{m_\alpha} + m_\alpha\omega_\alpha^2(X_\alpha - \frac{F_\alpha(Q)}{\omega_\alpha^2})^2]$ is the Hamiltonian of the bath of the harmonic oscillators that are coupled to the tagged particle [28]. Two parts in H_B are of physical interest: The first part is the ordinary harmonic oscillator; the second is the coupling term between the tagged particle position Q and the bath oscillator position X_α. The coupling function is taken to be linear in the displacement of the particle $F_\alpha(Q) = c_\alpha Q$, where c_α is known as the strength of the coupling between the tagged atom and the αth bath oscillator. Hence, there is a spectrum of coupling constants c_α by which each particle interacts with all other molecular degrees of freedom in the system. This spectrum of coupling strengths will play a major role in the subsequent analysis. The equation of motion for the tagged particle can then be derived straightforwardly, which leads to the following GLE:

$$\ddot{q} = -V'(q) - \int_{-\infty}^{t} \nu(t')\frac{dq}{dt'}dt' + q_e E_0 \sin(\omega t). \quad (1)$$

where the non-Markovian friction or memory kernel $\nu(t)$ is given by

$$\nu(t) = \sum_\alpha \frac{c_\alpha^2 m_\alpha}{\omega_\alpha^2 m}\cos(\omega_\alpha t). \quad (2)$$

Note we have converted into rescaled coordinates for standard normal-mode analysis: $q = Q\sqrt{m}$. This means $V(Q)$ and $V(q)$ are basically different functions. We have also redefined $q_e = e/\sqrt{m}$ as the (partial) reduced charge in rescaled coordinates. Then we can let the spectrum be continuous and c_α be a function of eigenfrequency ω_p, which leads to the following expression for the friction kernel:

$$\nu(t) = \int_0^\infty d\omega_p D(\omega_p)\frac{\gamma(\omega_p)^2}{\omega_p^2}\cos(\omega_p t), \quad (3)$$

where $\gamma(\omega_p)$ is the continuous spectrum of coupling constants, i.e., the continuous version of the discrete set $\{c_\alpha\}$ averaged over all tagged particles.

For any given (well-behaved) VDOS function $D(\omega_p)$, the existence of a well-behaved function $\gamma(\omega_p)$ that satisfies Eq. (3) is guaranteed by the fact that we can always decompose $\nu(t)$ into a basis of $\{\cos(\omega_p t)\}$ functions, by taking a cosine transform. The inverse cosine transform in turn gives the spectrum of coupling constants $\gamma(\omega_p)$ as a function of the memory kernel,

$$\gamma^2(\omega_p) = \frac{2\omega_p^2}{\pi D(\omega_p)}\int_0^\infty \nu(t)\cos(\omega_p t)dt. \quad (4)$$

This coupling function contains information on how strongly the particle's motion is coupled to the motion of other particles in a mode with vibrational frequency ω_p. This is important information because it tells us about the degree of long-range anharmonic couplings in the motion of the molecules.

B. Memory function modeling

Looking at Eq. (3), it is evident that the particle-bath Hamiltonian does not provide any prescription to the form of the memory function $\nu(t)$, which can take any form depending on the values of the coefficients c_α [28]. Hence, a shortcoming of particle-bath models is that the functional form of $\nu(t)$ cannot be derived *a priori* for a given system because, whereas the VDOS is certainly an easily accessible quantity from simulations of a physical system, the spectrum of coupling constants $\{c_\alpha\}$ is basically a phenomenological parameter.

However, for a supercooled liquid, the time-dependent friction, which is dominated by slow collective dynamics, has been famously derived within kinetic theory (Boltzmann equation) using a mode-coupling type approximation by Sjogren and Sjolander [29], and is given by the following elegant expression:

$$\nu(t) = \frac{\rho k_B T}{6\pi^2 m} \int_0^\infty dk\, k^4 F_s(k,t)[c(k)]^2 F(k,t), \qquad (5)$$

where $c(k)$ is the direct correlation function of liquid-state theory, $F_s(k,t)$ is the self-part of the intermediate scattering function (ISF) $F(k,t)$ [29]. All of these quantities are functions of the wave-vector k. Clearly, the integral over k leaves a time dependence of $\nu(t)$, which is controlled by the product $F_s(k,t)F(k,t)$. For a chemically homogeneous system, $F_s(k,t)F(k,t) \sim F(k,t)^2$, especially in the long-time regime.

From theory and simulations, we know that in supercooled liquids $F(k,t) \sim \exp[-(t/\tau)^b]$ for some τ and b when only α relaxation is present. When both α and β relaxations are present, the ISF has a two-step decay (one for α and one for β) [2]. It is easy to check that a two-step decay of the ISF within Eq. (5) is perfectly compatible with a memory function $\nu(t)$ given by a sum of two stretched-exponential terms.

Whereas the elegant relation by Sjogren and Sjolander Eq. (5) relies on mode-coupling type assumptions which may be questionable below T_g, we also point out that a more physically meaningful justification comes from its ability to generate an ISF $F(k,t)$ with a two-step decay in time for F112 upon taking $\nu(t)$ as a sum of two stretched exponentials, which is also compatible with the dielectric data (see the fittings below). This qualitative behavior for the ISF with a two-step decay has been demonstrated for the freon-112 system in simulations, e.g., Ref. [30], and in experiments [31]. Hence, despite the fact that the Sjogren and Sjolander relation relies on assumptions of mode-coupling type, the relationship between our memory function and the intermediate scattering function is physically meaningful and supported by data in the literature.

Hence, in light of the above discussion, we will take the following phenomenological expression for our memory function:

$$\nu(t) = \nu_0 \sum_i e^{-(t/\tau_i)^{b_i}}, \qquad (6)$$

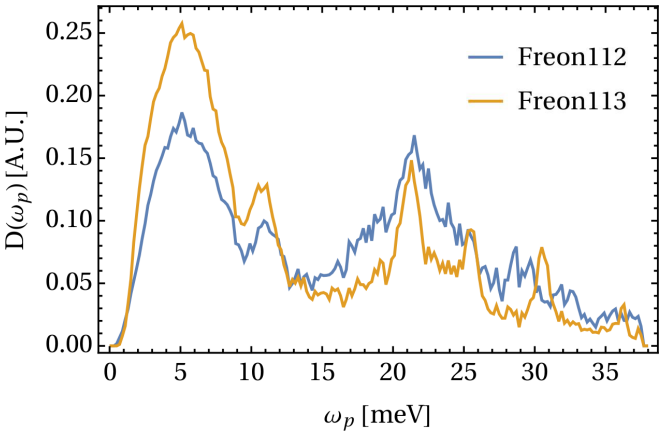

FIG. 1. Experimental VDOS for freon-112 (blue) and feon-113 (yellow). The data for freon-112 were published in Ref. [14], whereas the data for freon-113 were taken from Ref. [17].

where τ_i is a characteristic time scale with $i = 1$ for pure α relaxation and $i = 1,2$ for coexisting α and β relaxations. ν_0 is a constant prefactor.

C. Dielectric response and link with the VDOS

Following the same steps as those described in Ref. [20], upon taking the GLE Eq. (1) as the starting point, we obtain the complex dielectric function as

$$\epsilon^*(\omega) = 1 - A \int_0^{\omega_D} \frac{D(\omega_p)}{\omega^2 - i\omega\tilde{\nu}(\omega) - \omega_p^2} d\omega_p, \qquad (7)$$

where A is an arbitrary positive rescaling constant, ω_D is the Debye cutoff frequency (i.e., the highest eigenfrequency in the VDOS spectrum), and the tilde over ν denotes Fourier transformation. As one can easily verify, if $D(\omega_p)$ were given by a Dirac delta function, one would recover the standard simple-exponential (Debye) relaxation.

The VDOS is an important key input to the theoretical framework. The experimental VDOS were measured by means of inelastic neutron scattering using the direct spectrometer MARI of the ISIS facility (United Kingdom) and are shown in Fig. 1. The VDOS of F113 clearly exhibits a much more significant excess of low-frequency (boson-peak) modes with respect to F112 in the range of 2–5 meV.

For F113, we use only one stretched-exponential term in the memory function $\nu(t)$, hence $i = 1$ in Eq. (6). For F112, instead, $\nu(t)$ is the sum of two terms [$i = 1,2$ in Eq. (6)], both of which are stretched exponentials. The first term represents mainly the α process, although it also affects the β relaxation (hence the two are coupled as one can anticipate in the spirit of the Ngai coupling model [25]). The second term describes only β relaxation. Thus, the time scale of β relaxation is not identically equal to the time scale of the second stretched-exponential parameter, which is τ_2. This amounts to the fact that β relaxation is a process which is cooperative (hence coupled to α) and at the same time quasilocalized.

In terms of physical meaning, τ_1 represents the time scale of α relaxation, and the stretching exponent is related to the distribution of escape times from larger metastable basins in the glassy energy landscape. This is because the

TABLE I. Parameters of the memory function for freon-112.

Temperature	91 K	115 K	131 K
b_1	0.45	0.625	0.7
τ_1 (s)	0.558	3.12×10^{-7}	6.99×10^{-9}
b_2	0.2	0.56	
τ_2 (s)	1.55×10^{-2}	5.48×10^{-8}	
ν_0	4×10^{6}	3.9×10^{6}	6.3×10^{6}

stretched-exponential form arises from the integral average of simple-exponential decays weighted by a distribution of time scales; the broader the distribution, the lower the resulting stretching exponent [32]. Similarly, the second stretched exponential required to describe β relaxation is possibly related to the distribution of smaller wells within the same metabasin.

III. COMPARISON WITH THE EXPERIMENTAL DATA OF DIELECTRIC LOSS

Fitting parameters for F112 and F113 at different temperatures are listed in Tables I and II, and resulting fittings of the dielectric loss are displayed in Fig. 2.

For the fitting procedure, we have assumed that $D(\omega_p)$ and the overall scaling for the height of curve A are T independent.

IV. PHYSICAL MECHANISM OF SECONDARY RELAXATION

To physically understand the difference between F112 and F113, their dynamical coupling functions [Eq. (4)] have been analyzed (see Fig. 3). In general, the coupling spectrum decays from the highest Debye cutoff frequency of short-range high-frequency in-cage motions down to the low eigenfrequency part where the coupling goes up with decreasing ω_p towards zero due to phonons or phononlike excitations, which are collective and long wavelength and hence result in a larger value of γ.

There is a substantial difference between F112 and F113, especially in the middle part of the coupling spectrum where F112 shows much stronger coupling, which corresponds to medium-range correlated motions. This means that motions are strongly coupled also in the intermediate eigenfrequency domain where modes are typically quasilocalized, which corresponds to mesoscopic stringlike motions [33] typically associated with β relaxation [34]. In addition, the F113 spectrum is overall comparatively much lower in that energy regime, which clearly indicates that, for F113, the intermediate part of the coupling spectrum, i.e., the one of mesoscopic and stringlike motions, is scarcely populated, and one has a steep decay from the short-range high-frequency in-cage motions to the long-wavelength phononlike excitations with not much in between in the mesoscopic range. Hence in F113, the anharmonicity is much less prominent, and intermediate excitations are not important. This origin of the secondary relaxation aligns with the simulation results of Refs. [35,36], which point at the cooperative, although localized or quasilocalized, nature of secondary relaxation.

TABLE II. Parameters of the memory function for freon-113.

Temperature	72 K	74 K	76 K
b	0.26	0.3	0.35
τ (s)	7.133	0.326	2.38×10^{-2}
ν_0	8.28×10^{6}	7.28×10^{6}	6.28×10^{6}

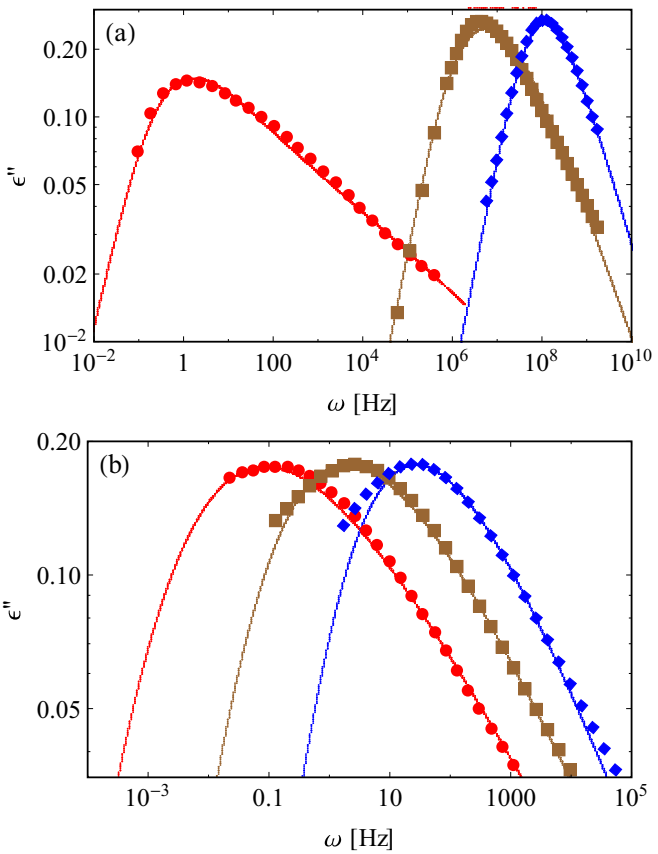

FIG. 2. Fitting of experimental dielectric loss data using the proposed theoretical model for (a) freon-112 at 91 K (red circles), 115 K (brown squares), and 131 K (blue diamonds) and for (b) freon-113 at 72 K (red circles), 74 K (brown squares), and 76 K (blue diamonds). The solid lines are the theoretical model presented here. A rescaling constant was used to adjust the height of the curves since the data are in arbitrary units. Experimental data for freon-112 were taken from Ref. [15], whereas the data for freon-113 were taken from Ref. [17].

This also gives insight into the difference in the form of the memory function used for the fittings of the two freons. Upon focusing on the integration in Eq. (4): The integral of $\nu(t)$ from 0 to ∞ increases from high ω_p (short range and fast vibration) to low ω_p (long range and slow vibration) since for slow collective vibration there is clearly much more extended friction due to contact between many particles all moving at the same time. Thus, the integral factor definitely contributes to the coupling being overall stronger for F112 than for F113. However, also the boson peak contributes to the coupling of F112 being larger than that of F113 [via the VDOS in the denominator of Eq. (4)] in the specific frequency range that corresponds to the boson peak. The boson-peak maximum [in $D(\omega)/\omega^2$, not shown] for both materials is on the order of 2 to

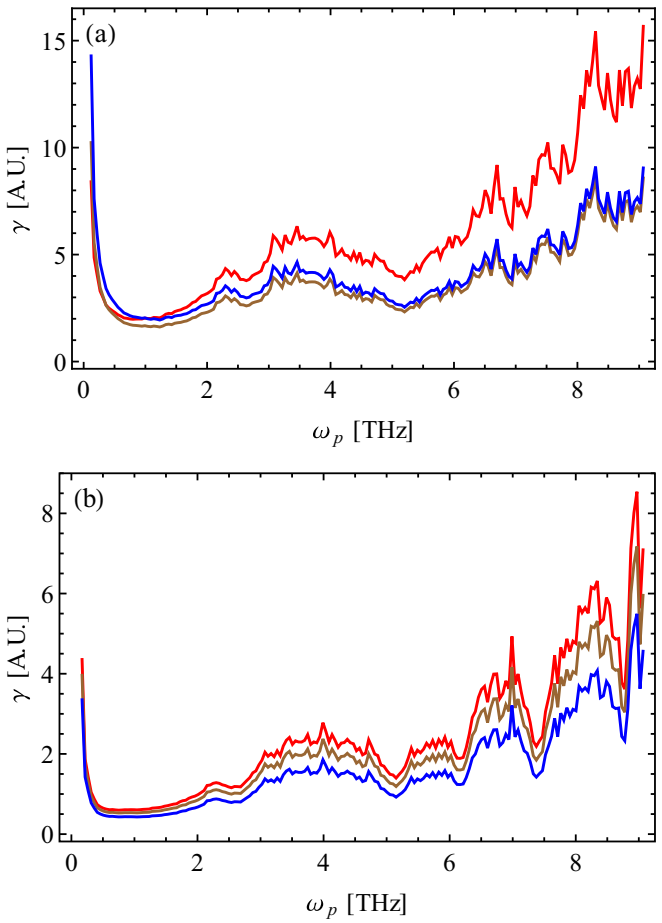

FIG. 3. Spectrum of coupling constants of (a) freon-112 and (b) freon-113 as a function of the vibrational eigenfrequency computed according to Eq. (4) using the phenomenological memory functions $\nu(t)$ used in the fitting of dielectric response in Fig. 2 with same color settings for the different temperatures. In (a), from top to bottom: 91 K, 131 K, 115 K, while in (b) from top to bottom: 72 K, 74 K, 76 K.

3 meV, i.e., ≈0.5–0.7 THz, which corresponds virtually to the lowest minimum in the coupling function (see Fig. 3) where, in addition, the minimum value is much lower for F113 (with a larger boson peak) than for F112. That means that in such a region not only we have larger dynamical coupling for F112 due to stronger medium-range correlations or anharmonicity, in general, but also we have the additional effect of the boson peak (soft weakly coupled modes, see Fig. 1) being smaller for F112 in that regime of vibrations.

As far as temperature effects on the coupling strength are concerned, we must point out first that, due to the fragility difference between the two freons, the temperature range in which fittings were performed is noticeably different. For F113 ($T_g = 71$ K) experimental dielectric functions are available at the highest reduced temperature of $T_r = 76/71 = 1.07$, whereas for F112 ($T_g = 90$ K) the highest value is around $T_r = 131/90 = 1.46$. Bearing this in mind, it can be noted that, upon increasing temperature, the "going up" tail at decreasing ω_p towards zero becomes smaller, which means less phononlike modes. In general, absolute coupling values shift down (lower coupling) with the increase in temperature as expected, and the decay of correlated motions from high ω_p to low ω_p becomes also somewhat steeper with increasing T.

V. DISCUSSION AND CONCLUSIONS

The stronger coupling between collective and individual motions for F112 could be a physical explanation, of why in the dielectric study of F112 in Ref. [15] the authors described so many problems to disclose α from β relaxation. For F112, collective vibrations, medium-ranged and slow motions are much more important than for F113 in such a way that individual molecular motions (β relaxation) should correlate, i.e., are much more coupled, with motions of surrounding molecules (collective motions associated with the α relaxation). And, even more, if slow vibrations are more important and more heterogeneous in F112, this should mean stronger coupling between collective and individual motions, so then, much more phonon scattering for F112 and, as a consequence, lower thermal conductivity for F112 than for F113 as has been experimentally shown (see Fig. 5 in Ref. [13]). In addition, it should be emphasized that the higher thermal conductivity for F113, analyzed in terms of the soft-potential model, was also attributed to the low coupling strength between sound waves and the soft quasilocalized modes. Moreover, the dynamical coupling function γ extends over a frequency range much broader than that of the boson peak, and thus the role of the boson peak is confined to a specific frequency range, which is around the minimum in the coupling spectrum. The fact that boson peak is stronger for F113 leads to a lower coupling in that region and contributes to the already lower coupling of F113 compared to F112 in that region. Because the boson peak is associated with soft modes, which "break" the coherence of phonons (hence more phonon scattering), it leads to even lower coupling in the boson-peak frequency range for F113.

In conclusion, we have presented an approach which makes it possible to directly link the vibrational density of states of orientational glasses measured experimentally with the macroscopic dielectric response and the underlying heterogeneous dynamics. Furthermore, the model effectively accounts also for the medium- and long-range anharmonic coupling among molecular degrees of freedom and allows one to disentangle α and β relaxations on the basis of the extent of dynamical coupling in different eigenfrequency sectors of the vibrational spectrum. The appearance of secondary β relaxation is associated with higher values of the dynamical coupling strength of correlated particle motions in the regime of mesoscopic quasilocalized motions (e.g., stringlike motions, vortices, etc. [34]) and is promoted by a lower excess of soft modes in the boson-peak frequency range.

In our model, we require two forms of stretched exponentials in the memory function in the generalized Langevin equation, hence two relaxation times, to fit both α and β relaxations. The β-relaxation process cannot be recovered with only one stretched exponential (i.e., with only one term in the memory function). One of the stretched exponentials dominates the α peak whereas the coexisting effect of two stretched exponential terms in the memory function gives rise to the β or secondary relaxation. In other words, the two terms of memory function both affect the secondary relaxation, whereas only one of them controls the α relaxation. This

implies that there is indeed a deep microscopic dynamical coupling between the two relaxation processes, which has not been unveiled so far. In future work this framework will be used to provide more microscopic insight into the dynamical nature of this coupling, also in the context of the Ngai coupling model [26].

ACKNOWLEDGMENTS

B.C. acknowledges the financial support of CSC-Cambridge Scholarship. J.L.T. acknowledges MINECO (Grant No. FIS2017-82625-P) and the Catalan government (Grant No. SGR2017-042) for financial support.

[1] P. Dean, The vibrational properties of disordered systems: Numerical studies, Rev. Mod. Phys. **44**, 127 (1972).
[2] E. Donth, *The Glass Transition: Relaxation Dynamics in Liquids and Disordered Materials* (Springer, Berlin/Heidelberg, 2001).
[3] L.-M. Martinez and C. A. Angell, A thermodynamic connection to the fragility of glass-forming liquids, Nature (London) **410**, 663 (2001).
[4] C. A. Angell, K. L. Ngai, G. B. McKenna, P. F. McMillan, and S. W. Martin, Relaxation in glassforming liquids and amorphous solids, J. Appl. Phys. **88**, 3113 (2000).
[5] K. L. Ngai, J. H. Magill, and D. J. Plazek, Flow, diffusion and crystallization of supercooled liquids: Revisited, J. Chem. Phys. **112**, 1887 (2000).
[6] F. Stickel, E. W. Fischer, and R. Richert, Dynamics of glass forming liquids. I. Temperature derivative analysis of dielectric relaxation data, J. Chem. Phys. **102**, 6251 (1995).
[7] J. Krausser, K. Samwer, and A. Zaccone, Interatomic repulsion softness directly controls the fragility of supercooled metallic melts, Proc. Natl. Acad. Sci. USA **112**, 13762 (2015).
[8] R. Boehmer, K. L. Ngai, C. A. Angell, and D. J. Plazek, Nonexponential relaxations in strong and fragile glass formers, J. Chem. Phys. **99**, 4201 (1993).
[9] C. A. Angell, Structural instability and relaxation in liquid and glassy phases near the fragile liquid limit, J. Non-Cryst. Solids **102**, 205 (1988).
[10] A. Drozd-Rzoska, S. J. Rzoska, S. Pawlus, and J. L. Tamarit, Dielectric relaxation in compressed glassy and orientationally disordered mixed crystals, Phys. Rev. B **74**, 064201 (2006).
[11] R. Brand, P. Lunkenheimer, and A. Loidl, Relaxation dynamics in plastic crystals, J. Chem. Phys. **116**, 10386 (2002).
[12] M. A. Ramos, S. Vieira, F. J. Bermejo, J. Dawidowski, H. E. Fischer, H. Schober, M. A. González, C. K. Loong, and D. L. Price, Quantitative Assessment of the Effects of Orientational and Positional Disorder on Glassy Dynamics, Phys. Rev. Lett. **78**, 82 (1997).
[13] G. A. Vdovichenko, A. I. Krivchikov, O. A. Korolyuk, J. L. Tamarit, L. C. Pardo, M. Rovira-Esteva, F. J. Bermejo, M. Hassaine, and M. A. Ramos, Thermal properties of halogenethane glassy crystals: Effects of orientational disorder and the role of internal molecular degrees of freedom, J. Chem. Phys. **143**, 084510 (2015).
[14] I. V. Sharapova, A. I. Krivchikov, O. A. Korolyuk, A. Jezowski, M. Rovira-Esteva, J. L. Tamarit, L. C. Pardo, M. D. Ruiz-Martin, and F. J. Bermejo, Disorder effects on heat transport properties of orientationally disordered crystals, Phys. Rev. B **81**, 094205 (2010).
[15] L. C. Pardo, P. Lunkenheimer, and A. Loidl, α and β relaxation dynamics of a fragile plastic crystal, J. Chem. Phys. **124**, 124911 (2006).
[16] K. Duvvuri and R. Richert, Dynamics of glass-forming liquids. VI. dielectric relaxation study of neat decahydro-naphthalene, J. Chem. Phys. **117**, 4414 (2002).
[17] A. Vispa, M. Romanini, M. A. Ramos, L. C. Pardo, F. J. Bermejo, M. Hassaine, A. I. Krivchikov, J. W. Taylor, and J. L. Tamarit, Thermodynamic and Kinetic Fragility of Freon 113: The Most Fragile Plastic Crystal, Phys. Rev. Lett. **118**, 105701 (2017).
[18] T. B. M. Domschke, M. Marsilius, and T. Voigtmann, Glassy relaxation and excess wing in mode-coupling theory: The dynamic susceptibility of propylene carbonate above and below Tc, Phys. Rev. E **84**, 031506 (2011).
[19] S. Albert, T. Bauer, M. Michl, G. Biroli, J.-P. Bouchaud, A. Loidl, P. Lunkenheimer, R. Tourbot, C. Wiertel-Gasquet, and F. Ladieu, Fifth-order susceptibility unveils growth of thermodynamic amorphous order in glass-formers, Science **352**, 1308 (2016).
[20] B. Cui, R. Milkus, and A. Zaccone, Direct link between boson-peak modes and dielectric α-relaxation in glasses, Phys. Rev. E **95**, 022603 (2017).
[21] G. P. Johari and M. Goldstein, Viscous liquids and the glass transition. II. Secondary relaxations in glasses of rigid molecules, J. Chem. Phys. **53**, 2372 (1970).
[22] K. L. Ngai, Correlation between the secondary β-relaxation time at T_g with the Kohlrausch exponent of the primary α relaxation or the fragility of glass-forming materials, Phys. Rev. E **57**, 7346 (1998).
[23] P. Lunkenheimer, U. Schneider, R. Brand, and A. Loid, Glassy dynamics, Contemp. Phys. **41**, 15 (2000).
[24] L. Yu, Amorphous pharmaceutical solids: preparation, characterization and stabilization, Adv. Drug Delivery Rev. **48**, 27 (2001).
[25] K. Ngai, Dynamic and thermodynamic properties of glass-forming substances, J. Non-Cryst. Solids **275**, 7 (2000).
[26] K. L. Ngai, Relation between some secondary relaxations and the relaxations in glass-forming materials according to the coupling model, J. Chem. Phys. **109**, 6982 (1998).
[27] D. A. Parshin, Interactions of soft atomic potentials and universality of low-temperature properties of glasses, Phys. Rev. B **49**, 9400 (1994).
[28] R. Zwanzig, Nonlinear generalized Langevin equations, J. Stat. Phys. **9**, 215 (1973).
[29] L. Sjogren and A. Sjolander, Kinetic theory of self-motion in monatomic liquids, J. Phys. C **12**, 4369 (1979).
[30] F. Affouard and M. Descamps, Analogy of the slow dynamics between the supercooled liquid and supercooled plastic crystal states of difluorotetrachloroethane, Phys. Rev. E **72**, 012501 (2005).
[31] F. Affouard, E. Cochin, F. Danede, R. Decressain, M. Descamps, and W. Haeussler, Onset of slow dynamics in

difluorotetrachloroethane glassy crystal, J. Chem. Phys. **123**, 084501 (2005).

[32] D. C. Johnston, Stretched exponential relaxation arising from a continuous sum of exponential decays, Phys. Rev. B **74**, 184430 (2006).

[33] C. Donati, J. F. Douglas, W. Kob, S. J. Plimpton, P. H. Poole, and S. C. Glotzer, Stringlike Cooperative Motion in a Supercooled Liquid, Phys. Rev. Lett. **80**, 2338 (1998).

[34] R. Richert, H.-B. Yu, and K. Samwer, Structural rearrangements governing Johari-Goldstein relaxations in metallic glasses, Sci. Adv. **3**, e1701577 (2017).

[35] P. Harrowell, Visualizing the collective motions responsible for the α and β relaxations in a model glass, Phys. Rev. E **48**, 4359 (1993).

[36] Y. Cohen, S. Karmakar, I. Procaccia, and K. Samwer, The nature of the β-peak in the loss modulus of amorphous solids, Europhys. Lett. **100**, 36003 (2012).